

Quantum Hall Metrology Samples and Their Use for Resistance Calibration

H. Bruus*

Danish Institute of Fundamental Metrology, Lundtoftevej 100, DK-2800 Lyngby, Denmark

and

P. E. Lindelof

Physics Laboratory, H. C. Ørsted Institute, Universitetsparken 5, DK-2100 Copenhagen Ø, Denmark

Received March 4, 1991; accepted June 18, 1991

Abstract

A measurement system capable of doing automated one to one quantum Hall effect calibration of ordinary wire wound standard resistors kept at room temperature has been constructed. The relative resolution of the system is 10^{-7} , but due to the lack of temperature stabilization of the standard resistors the total relative uncertainty is 10^{-6} . The quantum Hall samples used in the calibration are GaAlAs/GaAs heterostructures grown on the Molecular Beam Epitaxy system at the H. C. Ørsted Institute and also processed and mounted there. The quantum Hall samples are demonstrated to allow comparisons at least down to 2×10^{-9} level. Detailed description of techniques for sample preparation and measuring equipment are presented. Furthermore examples are given of the actual calibration of resistors as well as some concluding remarks about the calibration set-up, which is under construction at the Danish Institute of Fundamental Metrology.

1. The quantum Hall effect used in the maintenance of the ohm

Due to the discovery of two very accurate quantum effects, the Josephson effect and the quantum Hall effect, calibration to the highest level and accuracy has developed considerably in recent years [1, 2]. This development has important implication for trade and industry and is of concern to all industrialised countries and has been vigorously pursued in the Nordic countries [3]. In the following we shall describe Danish efforts to develop a resistance standard based on the quantum Hall effect. Although our calibration facility is still in progress, we believe that results on sample preparation, measurement techniques and calibration methods may be of interest to the scientific community within the fundamental metrology.

The electrical base unit within the international system of units, *Système Internationale d'Unités* (SI), is the ampere. From combinations of this unit with the three mechanical base units (the metre (m), the second (s), and the kilogram (kg)) all the other electrical units are derived. This, however, does not imply that the ampere is the unit which is the easiest to realize. In fact it is the farad, which for the time being can be realized with the highest accuracy of all electrical units by the so-called calculable capacitor [4]. The ohm is closely related to the farad by AC techniques, so the ohm can be realized better than the ampere. Up to January 1, 1990 most national metrology laboratories based their representation of the ohm on the mean resistance of a particular group of precision

wire-wound 1Ω standard resistors. A major problem with these standard resistors is ageing, a process which of course is not identical from one resistor to the other or from one laboratory to the other. The ageing would not be such a big problem, if it were easy to monitor the standards with a relative uncertainty of 10^{-7} by means of the calculable capacitor in regular time intervals. However, the complete calibration procedure is so tedious that only very few laboratories have been able to perform the complete calibration scheme based on the calculable capacitor [5]. Therefore, in practice, each country has had their own national representation of the ohm, and the differences between them have been significant. By the discovery of the quantum Hall effect [6] (QHE) this situation was changed. Figure 1 shows an example of the resistance per square, ρ_{xx} , as well as the transverse resistance ρ_{xy} , as a function of magnetic field for one of our MBE-grown samples, suited for quantum Hall calibration. The horizontal steps in the transverse resistance at $R_k/4$, $R_k/6$, $R_k/8$ etc. ($R_k = 25812.807\Omega$) are the so-called quantum Hall plateaus. From a metrologist's point of view the great virtue of the QHE is that a resistance standard based on a plateau has perfect reproducibility and constancy [7, 8]. No parameters such as temperature, geometry, time and location seems to influence the Hall resistance in an ideal QHE experiment. This reproducibility and constancy of the quantum Hall resistance is believed to be related to the fundamental constants h (the Planck constant) and e (the charge of the electron) by

$$R_k \cong \frac{h}{e^2} \quad (1)$$

For metrologists it really does not matter, whether h/e^2 has anything to do with the QHE, as long as the QHE only is going to be used for representing the ohm and not for realizing it. It is the constancy and the reproducibility of the plateaus in the QHE that are of metrological importance, and not specific values at the plateaus. Independent of the values of h and e but based on calculable capacitor calibrations the quantum Hall resistance was therefore by the *Comité International des Poids et Mesures* (CIPM) from January 1, 1990 frozen to have the following recommended value (the von Klitzing constant) and uncertainty [9]:

$$R_k: 25812.807\Omega$$
$$\text{Assigned standard deviation: } 0.005\Omega \quad (2)$$

* Present address: NORDITA, Blegdamsvej 17, 2100 Copenhagen Ø, Denmark.

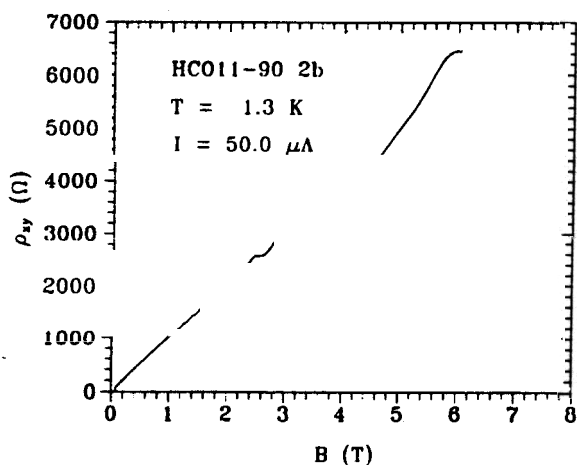
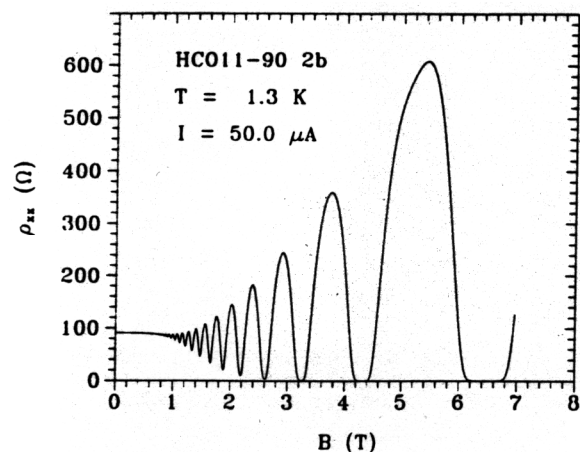


Fig. 1. Longitudinal resistivity ρ_{xx} and transverse (Hall) resistivity ρ_{xy} measured on a quantum Hall sample (see Fig. 2) as a function of magnetic field. Sample: HCØ11-90 2b. Temperature: $T = 1.3$ K, Current through Hall bar: $I = 50 \mu\text{A}$.

Relative standard deviation: 2×10^{-7}

It is important to emphasize that the new recommendations concerning the ohm and the volt does not constitute a redefinition of SI units. For example the ohm is still defined by the relation $1 \Omega = 1 \text{ m}^2 \text{ kg}^1 \text{ A}^{-2} \text{ s}^{-3}$ thereby maintaining its connection to the mechanical units, and it is still most accurately realized using the calculable capacitor. However it can now more easily be represented by the use of the quantum Hall effect with an assigned relative standard deviation of 2×10^{-7} . By these recommendations a world wide uniform representation of the ohm is guaranteed. In Denmark work began in 1987 in order to achieve a representation of the ohm unit based on the quantum Hall effect. In the nearest future it will be implemented as a calibration service by the Danish Institute of Fundamental Metrology (DFM) [10].

2. Preparation of quantum Hall samples

The quantum Hall samples are made on the basis of epitaxially grown GaAs/Ga_{1-x}Al_xAs heterostructures. The interface between GaAs and Ga_{1-x}Al_xAs is abrupt and planar – an essential prerequisite for the formation of a 2-dimensional electron gas (2DEG). Stringent requirements for the quality of both the growth and the processing of the samples must be met before their metrological use [11]. It has turned out to be occasionally difficult to obtain samples [12] and to our knowledge the MBE-grown GaAs/Ga_{1-x}Al_xAs heterostructures

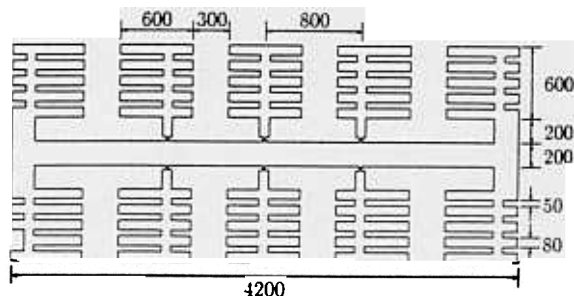


Fig. 2. The geometry of a quantum Hall sample. The pattern is mesa-etched into the GaAs/GaAlAs heterostructure surface. The 4 current contact areas and 6 voltage contact areas are made with a long circumference in order to facilitate contacting and to make sure that the highly doped contact regions overlap the edges of the mesa, which is a precondition for maintaining contact in high magnetic fields.

produced at the MBE-Center at the H. C. Ørsted Institute are the first samples in the Nordic countries suitable for calibration of resistors to the highest level of precision.

The heterostructures were made by using molecular beam epitaxy (MBE) – an ultra high vacuum evaporation technique in which molecular or atomic beams consisting of typically As₂, As₄, Ga or Al impinges upon a rotating substrate maintained at a high temperature, whereby the Ga, Al and As atoms are deposited. The beams are generated by Knudsen effusion cells emitting fluxes of molecules or atoms. These fluxes are controlled by temperature regulation of the cells and by shutters in front of the cells. We used a Varian Gen II MBE system for our growth of heterostructures. The layer sequence was from top to bottom: 0.5 mm GaAs substrate, 1 μm GaAs buffer layer, 10 nm Ga_{0.7}Al_{0.3}As spacer layer, 60 nm Si-doped ($2 \times 10^{18} \text{ cm}^{-2}$) Ga_{0.7}Al_{0.3}As barrier layer and a 5 nm GaAs cap layer. The two important parameters, which characterize such samples namely mobility and carrier density in the two-dimensional electron gas. The carrier density must match the filling factor of the chosen Hall plateau and the maximum magnetic field available. One way of tailoring the samples to a particular quantum Hall calibration set-up is by implanting the heterostructures with helium [13].

The first step in the device production is to design the geometry of the sample. We use a long rectangular shape with current leads at the ends and voltage probes at the sides. As shown in Fig. 2. the length-to-width ratios W/L are either 4 or 8 for our samples.

The procedure for the sample preparation is as follows: A 1.5 μm thick layer of positive Photo-Resist (1350 H) is used. The next step is wet-etching of the sample using H₃PO₄:H₂O₂:CH₃OH (1:1:3, etching 1 μm in 30 s). As a result of the etching at 1 μm high mesa, shaped as the photo mask, emerges on the surface of the sample. Since the 2DEG is situated less than 0.1 μm from the top of the mesa, we thereby define the 2DEG. The next step in the device fabrication is to make ohmic contacts to the 2DEG. First the sample surface has to be cleaned thoroughly to remove grease. This is done by using the following four chemicals in the given order: trichloroethene (C₂HCl₃), acetone (CH₃COCH₃), methanol (CH₃OH), and deionized water. Each chemical is poured into a separate 50 ml beaker, and the beakers are placed in an ultrasonic bath. The sample is cleaned for 60 s in each beaker, and after the final rinse it is lowered into ammonia water, NH₄OH:H₂O (1:15), for 15 s

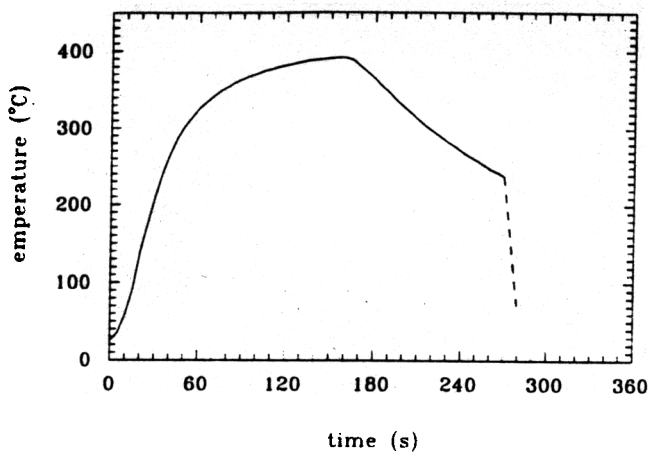


Fig. 3. Readings of the Bio-Rad furnace thermometer during the contact alloying of the 10 tin beads placed on the mesa shown in Fig. 2 as a function of time. The solid line indicates actual readings, while the dashed line symbolizes the rapid cooling of the sample after it is taken out of the furnace.

to remove oxides from its surface. The sample is then ready to have contacts mounted. We use two methods for contacting: Sn-bead-contacts and Au-Ge-Ni-contacts, but since the Sn-bead contacts have the lowest resistance only these will be described here. The Sn-beads are disk-shaped pieces of 99.9% pure tin with a diameter of $500\ \mu\text{m}$ and a thickness of $20\ \mu\text{m}$. Immediately after the rinsing of the sample, it is placed on the heater-stage on a Bio-Rad RC 2400 Polaron alloying furnace, where it can be observed during the heat treatment by a microscope. One Sn-bead is placed on each of the 10 square contact areas ($600\ \mu\text{m}$ by $600\ \mu\text{m}$, see Fig. 2). This is done by pressing a hand held needle into one of the Sn-beads until it sticks to the needle. To clean the surface of the Sn-bead the needle with the attached Sn-bead is lowered for 3 s into the HCl-vapors in a glass containing concentrated liquid HCl. Observing through the alloy furnace microscope the Sn-bead is placed on the contact area by jiggling a bit with the needle by the help of another needle until the Sn-bead falls down on the mesa. Then the Sn-bead is flattened on the mesa by pressing it with the two needles. It takes about 2 minutes to place all 10 Sn-beads on the 10 contact areas. The alloy furnace is then closed without touching the sample, and for about 20 minutes reducing formier gas ($\text{N}_2:\text{H}_2, 9:1$) is lead through the furnace to remove as much oxygen as possible. Without interrupting the flow of the formier gas through the furnace, the heater of the furnace is then activated. The temperature development of the alloying is as shown in Fig. 3. During the alloying process, Sn atoms from the Sn-beads are diffusing down through the cap layer, the donor layer and the spacer layer and finally reach the 2DEG in the buffer layer. This trace of Sn atoms presumably constitutes an ohmic contact leading from the surface of the sample down to the 2DEG. The reason for making the cuttings in the shape of the contact area as seen in Fig. 2, instead of leaving them just as plain squares ($600\ \mu\text{m}$ by $600\ \mu\text{m}$), is the following: during the heating, but before the alloying process begins, the Sn-beads contracts from the disk-shape to a sphere with a diameter around $80\ \mu\text{m}$. If no cuttings were made they would roll around and finally settle in an unpredictable position inside the contact area or maybe even roll down from the mesa. By making the cuttings we obtain two things: (1) the Sn-bead is caught in one of the internal corners of the contact area and stays on the mesa, and (2) the Sn-bead lies on the edge of the

mesa. When doing electrical measurements in high magnetic fields, it is crucial that the electrical contacts are at the edges of the sample, because otherwise, due to the large Lorentz-force and the almost vanishing conductivity, σ_{xx} , the electrons would go around the contact, unable to enter it. It would thus be almost impossible to drive any current through the sample or measure any voltages across it; one can speak of unintentionally having obtained a Corbino geometry.

The final step in the device fabrication is to mount the device on a chip carrier which fits into the experimental equipment. With a tiny drop of epoxy the individual device is glued to a Dual-In-Line 14 legs chip carrier equipped with AgPd thick film leads. By the means of an ultrasonic gold ball bonder, the device contacts and the leads of the chip carrier are connected (see Fig. 4). We emphasize two aspects of the bonding procedure, which it has taken some time to optimize. Firstly that during the bonding the temperature of the sample was 120°C . Secondly that the ball bonder tip hits the Sn-bead with such a force that it sinks half way down into the semi sphere shaped Sn-beads. If this force is too little, the gold wire will not stick to the Sn-bead, and if it is too strong the Sn-bead can be so badly demolished that it is torn off the sample. The typical device ready to use is shown in Fig. 4.

3. Test on the samples

The first test to be performed on a sample is to check if all the contacts are working at room temperature. The sample under test is placed in the sample holder so that no light can hit the sample, whereby disturbing photoelectric effects are avoided. A test current is supplied from a Keithley 220 programmable current source via the current leads, and six various voltage differences are measured using a Keithley 181 nanovoltmeter. The voltage measurements are found from several measurements with both positive and negative current polarity. If all voltage drops at the two sides of the sample are identical, the sample is characterized as being adequate, and ready to be inserted into the cryostat.

Out of 30 samples made by the procedure above and measured at low temperatures and in high magnetic fields 95% had contacts, which were adequate at low temperatures and in high magnetic fields. It is of great help that a successful test carried out on a sample at room temperature is an almost certain guarantee of the quality of the sample, because then wasted tests at cryogenic temperatures can be avoided. National Institute of Metrology (NIM) China [14] and Statens Provningsanstalt (SP) Sweden [15], have reported excellent high precision calibration results based on our samples, and we offer collaboration with other metrology institutes as well.

To assure thermal equilibrium during the cool down the sample is lowered very slowly into the cryostat, a procedure that takes at least 10 minutes. It is also important to prevent any photo processes (e.g., persistent photoconductivity) to occur, when the sample is cold. If, as it usually is the case, the sample passes the contact test at 4.2 K, curve traces are taken of the magnetoresistivity, ρ_{xx} , and the Hall resistivity, ρ_{xy} , as shown in Fig. 1. With these curves a good feeling is obtained for the quality of the sample. The carrier concentration, n , is determined from the Shubnikov-de Haas oscillations and the Hall effect. These two values of n are normally in very good agreement. Together with the zero magnetic field value of

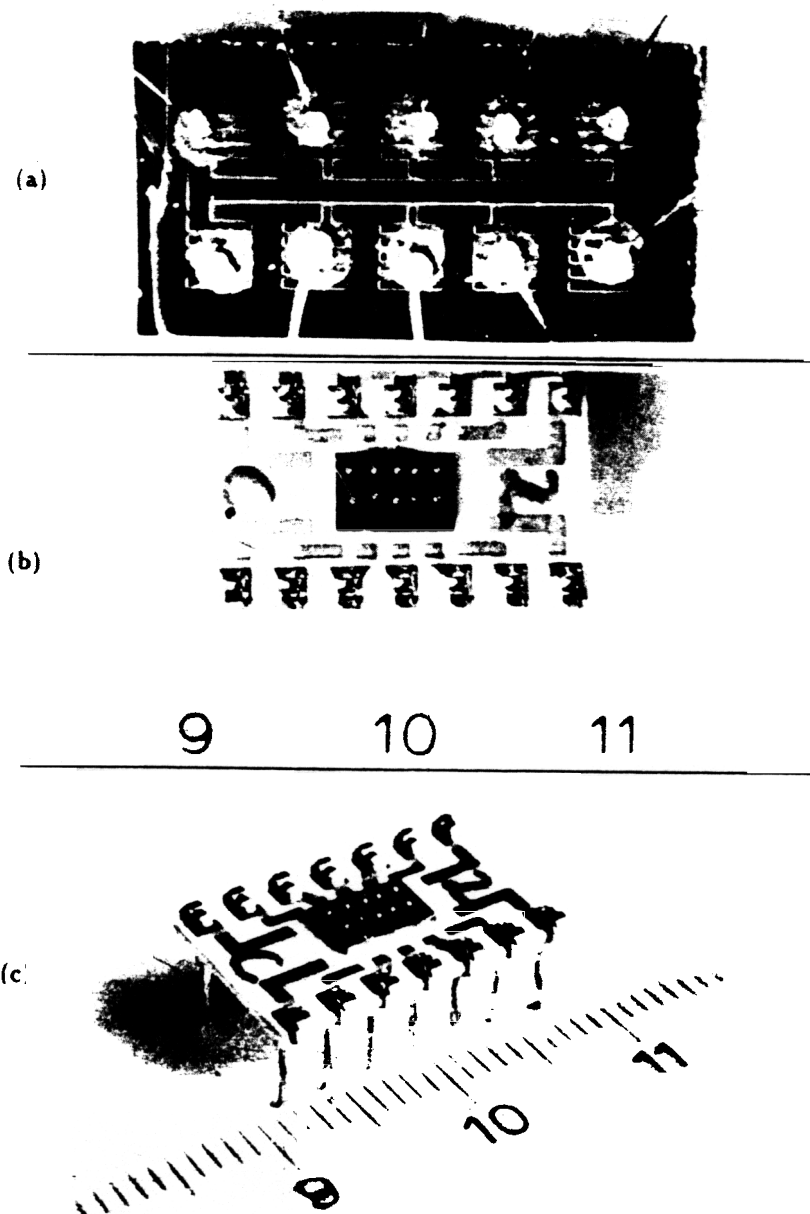


Fig. 4. Quantum Hall sample mounted on chip carrier. (a) close-up of the mesa structure and the 10 tin beads alloyed to the contact areas. (b) and (c) chip carrier showing gold bonding wires from the tin beads to the silver-palladium contact areas on the alumina chip carrier. The chip carrier is non-magnetic and designed for the quantum Hall samples. The smallest divisions on the scale are mm.

ρ_{xx} , n yields the zero magnetic field value of the electron mobility μ . The values of n and μ are determining parameters for the use of a given sample as basis for a QHE resistor. The optimal mobility is still a matter of debate [13], whereas the optimal value of the electron density depends on the magnetic field available and the QHE plateau under consideration. However, n should be less than the critical density, n_c , where the second sub-band begins to be populated to avoid the influence of inter subband scattering. In order to base our quantum resistor on the Hall plateau $i = 4$ we require 2DEGs with n as close to n_c as possible.

4. The principle of resistance comparisons

Together with the CPIM value of the von Klitzing constant, as already explained, it has been decided from January 1, 1990, to use the quantum Hall effect to establish a reference standard of resistance having an estimated one-standard-deviation relative uncertainty with respect to the ohm of

2×10^{-7} . The main goal of the quantum Hall metrology is therefore to compare the quantized Hall resistance with an ordinary standard resistor kept at room temperature. As a result of such a comparison the standard resistor is calibrated in absolute SI-units, and it can thus be used as a transfer standard, whereby the dissemination of the ohm is established.

It requires a special measurement system to carry out the comparison mentioned above. Only a few different systems has been used by the various national metrology laboratories. The principles of these systems are reviewed in [7, 8]. One of these systems is the potentiometric one-to-one calibration system described below, by which it is possible to compare a quantized Hall resistor with a standard resistor having nominally the same value. The basic principle of the potentiometric method is shown in Fig. 5. The standard resistor, R_w (w for wire wound), is placed in series with the quantum Hall resistor, R_H . Here, and in the following, one should imagine that the quantum Hall device is put in a state where Hall

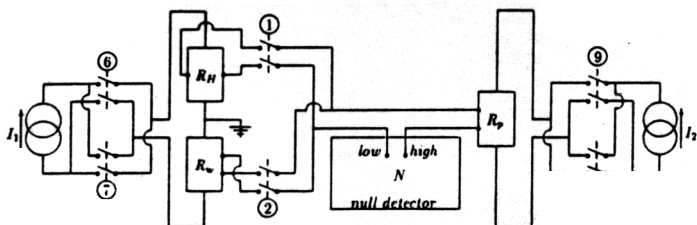


Fig. 5. The quantum Hall measurement system. R_H is situated in the helium cryostat, while the rest of the system is inside a shielded room. The metal cryostat is made part of the shielded room by use of a flexible metallic tube. The switches 1, 2, 6, 7, 9 and 10 are pneumatically operated from outside the shielded room. The null detector output is filtered on its way out of the shielded room.

plateau i is in existence. It would therefore be more correct to write $R_H(i)$. In all the metrological measurements described in the following $i = 4$ was used, and hence $R_H = 1/4R_K = 6453.202 \Omega$. R_w is designed to have nominally the same value. If no leakage currents are present, the current through R_H and R_w is the same (in practice $50 \mu A$), and therefore the voltages developed over the two resistors, are nearly the same (in practice $0.3 V$). The difference between these voltages is measured by a potentiometer consisting of a null detector, N , which measures small voltage differences, and a resistor, R_p (p for potentiometer), through which a current, I_2 , is passed so that the voltage drop, $R_p I_2$, is as close as possible to $R_H I_1$. By actuating switch no. 1, 6 and 9 in Fig. 5 the null detector measures the voltage difference $N_1 = R_H I_1 - R_p I_2$, which in practice is less than $30 \mu V$. In the switch position no. 2, 6 and 9 the voltage difference $N_2 = R_w I_1 - R_p I_2$ is measured. By subtraction of the two null detector signals the potentiometer voltage can be eliminated: $N_1 - N_2 = (R_H - R_w) I_1$. Now, since both N_1 and N_2 are small, even a quite crude measurement of I_1 yields a good calibration of

$$R_w = R_H - (N_1 - N_2) I_1. \quad (3)$$

To eliminate thermal emfs one must be able to change the current polarities, since such changes do not affect the thermal emfs but reverse the sign of the voltages $R_H I_1$, $R_w I_1$, and $R_p I_2$. During the measurements to be presented we use four null detector symbols $N(1+)$, $N(1-)$, $N(2+)$ and $N(2-)$ corresponding to the following four switch actuations respectively: (1, 6, 9), (1, 7, 10), (2, 6, 10) and (2, 7, 9). The numbers "1" and "2" refer to measurements on R_H and R_w respectively (switch no. 1 and 2). The signs refer to the current polarities (switch no. 6 or 7 and 9 or 10). For each of the four switch positions, the corresponding null detector signal is measured. When switch 1 is on, there will generally appear a thermal emf and likewise, when switch 2 is on. By the following expression for the wanted value of the wire wound resistor the thermal emfs and the potentiometer voltage, $R_p I_2$, are eliminated:

$$R_w = R_H \left(\frac{N(1+) - N(1-) + N(2+) - N(2-)}{2I_1 R_H} \right) \quad (4)$$

5. The metrology set-up

The complete metrology system is shown in Fig. 6. The system can be divided into three subsystems: the cryostat with the quantum Hall device, the shielded room with the

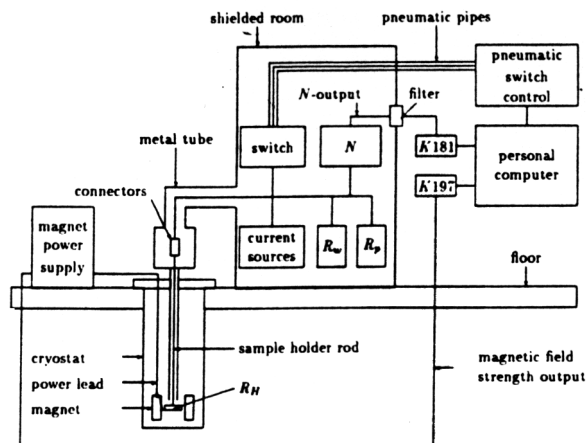


Fig. 6. The complete metrological system. The relative positions of the magnet power supply, the cryostat, the shielded room and the computer are shown. The electric circuit is here shown in a block diagram with indications of which parts of the system are inside the shielded room. K181 and K197 are digital voltmeters. N is the null detector. R_H is the quantum Hall resistor. R_w and R_p are wire wound standard resistors.

measurement system, and the data acquisition equipment outside the shielded room. Now follows a description of these three parts of the system.

a. The cryostat

At cryogenic temperatures there are no severe problems with electrical leakage resistance, but as the leads approach room temperature greater care has to be taken. Special cables had to be chosen to lead from the sample holder at 1.3 K to the top of the cryostat at 300 K. Since the cryostat is made of metal it is not necessary to use shielded cables inside the cryostat. 8 silver plated single cables (2 for current leads and 6 for potential probes) was mounted on the sample holder rod and had PTFE (PolyTetraFluoroEthylene) insulation. The 8 single cables were soldered to the chip socket shown in Fig. 4 with ordinary Sn-solder. To ease change of samples connectors were placed at the top of the cryostat, in spite of the fact that it would have been better, if the cables were taken directly from the chip socket to the instruments in the shielded room. Three requirements were to be fulfilled: firstly, they must have a high leakage resistance. Secondly, they must not produce to high thermal emfs. And thirdly, they must be vacuum tight. Connectors produced by LEMO having gold plated contact pins and PTFE insulation met all three requirements. The cables leading from the connectors on top of the cryostat to the instruments inside the shielded room were shielded PTFE-insulated twisted pairs of 0.5 mm diameter silver plated copper. The total length of the cables connecting the quantum Hall device with the instruments inside the shielded room was 4 m. The total electrical leakage resistance of the cables was measured to around $10^{13} \Omega$ leading to a relative error as small as $R_K/10^{13} \Omega \approx 10^{-9}$.

b. The shielded room

To create an electrically calm environment for the metrological measurements a shielded room was constructed. Shielding is important because mixing of radiofrequencies or clock-frequencies of computers in any non-linear contact will create error signals at d.c., which will deteriorate the metrological measurement. A metal tube connected the shielded room with the top of the cryostat. The copper foil of the shielded room

was used as common ground for the metrological measurement system as indicated by the ground symbol in Fig. 5. The shielding of the cables, of the current sources and of the switches were all taken to the same point. Thus avoiding any annoying ground loops.

A vital part of the metrological measurement system are the switches, which allows one to change the polarity of the currents, and to switch the potentiometer forth and back between the Hall device and the standard resistor. We used 2 Guildline's Low Thermal Selector Switches (9145A). The thermal emfs generated by the switches are less than 10 nV. This was in relative measure less than 3×10^{-8} of the signal and was therefore not a problem. For switching the selector switch pneumatically driven pistons were used. Thereby we avoided an extra galvanic inlet through the walls of the shielded room.

To obtain stable and low noise current sources a battery driven Hg-cell stabilized operational amplifier was used. To enhance the stability of the current sources 100 mAh was drained out of a total of 1000 mAh of the Hg-cells before mounting them. Furthermore special precision bulk foil resistors from Vishay were the main part of the controlling input resistor of the operational amplifier. The current sources gave about 50 μ A. As the current sources were not completely stable, it was necessary to adjust the value of R to about 10^{-4} in relative measure. Thereby it was also possible to tune the potentiometer voltage $R_p I_2$ to, for example, the Hall voltage $R_H I_1$.

The standard resistor R_w and the potentiometer resistor R_p of Fig. 5 were of the same kind. They were both high quality wire wound Wilkins standard resistors manufactured by Tinsley in U.K. They had the same nominal value, 6453.2 Ω , corresponding to the value of the quantized Hall resistance at plateau $i = 4$. If the currents I_1 and I_2 are tuned to be nearly identical, as described in the previous section, only quite minute voltage differences have to be measured by the null detector. We used three standard resistors from Tinsley denoted R_{75} , R_{76} and R_{78} each provided with a test certificate traceable to the British National Physics Laboratory (NPL).

The null detector employed in the measurements was a D.C. nanovoltmeter model N1a manufactured by EM Electronics. It is battery operated from internal chargeable batteries and has the advantage of complete electrical isolation. The null detector analog output was read electronically through a low pass filter. Even a good null detector with a high insulation resistance between "high" and "guard" could actually have a relatively poor insulation resistance between "low" and "guard" [16]. To avoid this it suffices to ensure that "low" is always as close as possible to the ground potential. However, in the case of R_H it requires specific knowledge of how the QHE sample is situated relative to the magnetic field to choose the correct low potential voltage probe [10].

c. Data acquisition

The basis of the data acquisition system consisted of an IBM Personal Computer AT equipped with an IEEE-interface (General Purpose Interface Bus Adapter) and a DAC-interface (IBM Personal Computer Data Acquisition and Control Adapter). The computer was used for three purposes: Firstly, it could read the null detector output via an IEEE-equipped Keithley 181 digital nanovoltmeter (denoted K181 on Fig. 6). Secondly, it could read the magnetic field strength output via

an IEEE-equipped Keithley 197 digital microvoltmeter (denoted K197 on Fig. 6). And thirdly, using the output terminals of the DAC-interface it controlled the 10 magnet valves of the pneumatic switch control. A typical measurement program consisted of the following routines: (1) set the switches using the DAC-controlled pneumatic switch system. (2) Wait a while for the system to settle down. (3) Read the strength of the magnetic field via the K197. (4) Read (maybe several times) the null detector via the K181, and read the time on the internal clock of the computer for each of these readings. (5) Repeat the whole scheme with new switch settings. The raw data of each reading is stored in specific data files, which then later can be used as the basis for a data analysis.

6. Accuracy of the quantum Hall effect

After the zero field test have been performed, and the ρ_{xx} and ρ_{xy} vs. magnetic field traces have been recorded, the magnetic field is set at the value corresponding to the centre of a QHE plateau $i = 4$. The centre of a plateau is found by monitoring the minimum ρ_{xx} while slowly varying the magnetic field at a temperature where the minimum ρ_{xx} is measurable. A current of approximately 50 μ A is passed through the sample. When an electrical current is passed through a sample in the QHE regime, the current flows from one corner of the sample to the diagonal opposite. As a consequence of this particular current flow the quantized Hall voltage does actually appear between the two current leads. When the voltage drop between the two current leads is measured, it will therefore consist of contributions not only originating from the resistance of the attached wires and from the contact resistance, but also from the Hall resistance. The resistances of the attached wires have been determined by the use of an empty chip carrier having all its AgPd-pads connected to each other with the same type of gold wire as are used to connect a quantum hall sample. This dummy sample was inserted in the system and cooled to 4.2 K just as an ordinary sample. For a pair of wires the total resistance is $R_{\text{wire}} = 5.4 \Omega$. The resistance between the current leads resistance and any of the "pure" quantum hall resistances, amounts typically to 5.5 Ω . Since this difference equals the sum of the wire resistance, R_{wire} , and the contact resistance, R_{contact} , we can find the latter to be $R_{\text{contact}} \approx (0.1 \pm 0.1) \Omega$. The measured contact resistance is below the limit suggested in the technical QHE guidelines [11] to define the upper limit for an acceptable contact resistance. Our Au-Ge-Ni contacts had a resistance of about 1 Ω , but it has recently been demonstrated that such contacts can have much smaller contact resistance [17].

Before a calibration measurement can begin, the quality of the quantum Hall sample must be estimated following the empirical equation [18]:

$$\rho_{xy} = \frac{1}{i} R_k - \alpha \rho_{xx}, \quad |\alpha| < \quad (5)$$

where α is a phenomenological parameter, typically $\alpha \cong 0.2$. For application within metrology it is therefore important that ρ_{xx} is sufficiently small so that ρ_{xy} can be approximated by $(1/i)R_k$. To experimentally confirm this the null detector is connected directly to two of the longitudinal voltage probes. To eliminate thermal e.m.f.s the current polarity is

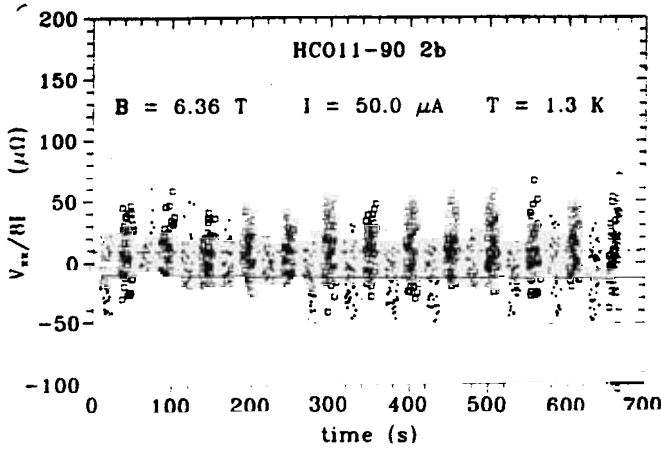


Fig. 7. Resistivity measurements at the centre of the plateau $i = 4$. The reason that $V_{xx}/8I$ has a divisor 8 is that the resistivity is measured along 8 squares (see Fig. 2). The experimental results are plotted as respectively small squares and small dots representing opposite current polarity. The weighted average is $\rho_{xx} = 9.5 \mu\Omega$. An emf-induced offset of $2.1 \mu\text{V}$ is outbalanced by appropriate setting of the null-detector.

changed, and the corresponding null detector readings are acquired through the IEEE-bus system.

In the following examples resistivity measurements on sample HCO11-90 at Hall plateau $i = 4$ ($B = 6.36 \text{ T}$) are shown. The measurement in Fig. 7 the scheme consists of several repetitions of the following cycle: (1) change of current polarity, (2) 10 seconds rest, (3) 15 seconds of measurements during which 50 voltage values are read. When the current polarity is positive and negative respectively, the resistivities $r_{xx}(+I) = V_{xx}/|+I|$ and $r_{xx}(-I) = V_{xx}/|-I|$, which include induced thermal e.m.f. offset, are measured. Whereas at 4.2 K the true resistivity is several $\text{m}\Omega$, it became negligibly small as soon as the temperature was lowered to 1.3 K and the results showed in Fig. 7 emerges. Since $r_{xx}(+I)$ and $r_{xx}(-I)$ both are roughly equal to the e.m.f. induced offset, it is possible to use the offset-option on the null detector and consequently obtain a high resolution on the null detector. According to the regression analysis the drift rates are less than $20 \text{ n}\Omega/\text{s}$ and hence negligible. At 1.3 K the true resistivity, ρ_{xx} , and the e.m.f., $V_{\text{e.m.f.}}$, are then:

$$\rho_{xx} = \frac{1}{2}(r_{xx}(+I)) - r_{xx}(-I) = (9.5 \pm 2.4) \mu\Omega + 0.02 \mu\Omega/\text{s} \cdot t \quad (6)$$

$$V_{\text{e.m.f.}} = 2.1 \mu\text{V}$$

According to eq. (5) a small finite value of ρ_{xx} can lead to deviations in ρ_{xy} from the ideal value $R_H/4$. These relative deviations are less than ρ_{xx}/ρ_{xy} , and in the actual case the upper bound of the deviations is of the order:

$$\frac{\rho_{xx}}{\rho_{xy}} = \frac{9.5 \cdot 10^{-9} \Omega}{6453 \Omega} \approx 10^{-9}. \quad (7)$$

The peak-to-peak noise level in Fig. 7 is about $0.1 \text{ m}\Omega$ which corresponds to 20 nV . This noise level is too high to be explained by a Johnson-noise calculation for a 6453Ω resistor using the null detector band width of 4 Hz , or by the noise of the null detector itself, which is only 3 nV . The major noise source is most likely the current sources. It was possible to change the noise level by changing the operational amplifiers of the current sources. The current sources are no doubt the weakest point in the present system as regards the random noise.

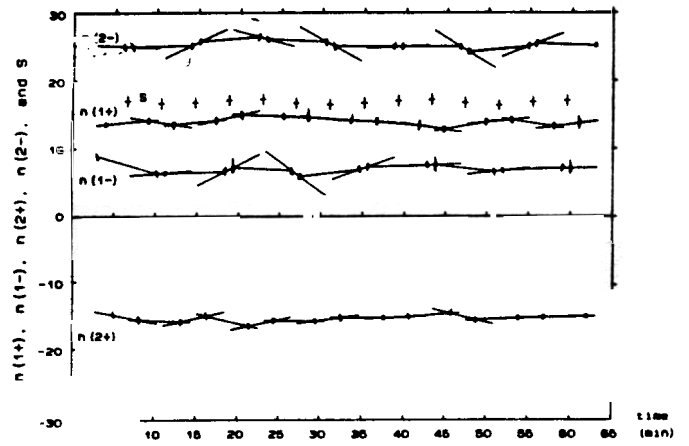


Fig. 8. Measurements of the null detector signals $n(1+)$, $n(1-)$, $n(2+)$ and $n(2-)$ in units of parts per million in a comparison between a wire wound resistor and the quantum Hall resistor. To calculate $S = -0.5(n(1+) - n(1-) + n(2+) - n(2-))$ one linear regression has been performed for each of the time symmetric sub-sequences, and the resulting regression lines have been drawn. On the graph 14 sub-sequences have been completed, and the resulting 14 values of S are marked with crosses.

7. Calibration of the wire wound resistors

When all the tests on the quantum Hall sample have been performed with success, the stage is set for the calibration measurements of the wire wound resistors R_{75} , R_{76} and R_{78} . The magnetic field is set at the plateau centre value. Just before starting the calibration program, the current, I_1 , through the series connection of the quantum Hall sample and the standard resistor, R_w , is determined to a relative uncertainty of 2×10^{-4} . This current implies a Hall voltage of $I_1 \times R_H(4)$. The calibration is performed at 1.3 K and at the QHE plateau $i = 4$ at $B = 6.36 \text{ T}$. The resistance of R_w can be calibrated according to eq. (4). If we write the current as $I_1 = I \pm \delta I$, where δI is the uncertainty of the measured current, we can introduce the relative null detector signals, $n(\dots)$, defined as the true null detector signals, $N(\dots)$, divided by the Hall voltage: $n(\dots) \equiv N(\dots)/(IR_H(4))$. Equation (4) leads us to define the sum S of relative null detector signals

$$S \equiv -\frac{1}{2}(n(1+) - n(1-) + n(2+) - n(2-)). \quad (8)$$

The sum S is a quantity defined by a measurement, and it must therefore be ascribed an uncertainty δS . Equation (4) for R_w can therefore now be rewritten as

$$R_w = R_H(4) \left(1 + \frac{S \pm \delta S}{1 \pm \delta I/I} \right) \approx R_H(4) \left(1 + S \pm \delta S \pm S \frac{\delta I}{I} \right) \quad (9)$$

According to (8) and (9) we need in principle to determine all four different $n(\dots)$'s at the same time in order to determine S and thereby calibrate R_w . We measure the four $n(\dots)$'s in the following repeated computer controlled symmetric sequence as a function of time:

$$|n(1-)n(1+)n(2+)n(2-)|n(2-)n(2+)n(1+)n(1-)|, \quad (10)$$

and we then do a linear regression for each consecutive pair of the same kinds of $n(\dots)$'s. In Fig. 8 an example of a measurement following the scheme eq. (10) is shown. In Fig. 8 this procedure has been carried out 14 times, and the resulting 14 values of $S \approx (R_w - R_H(4))/R_H(4)$ are marked by the

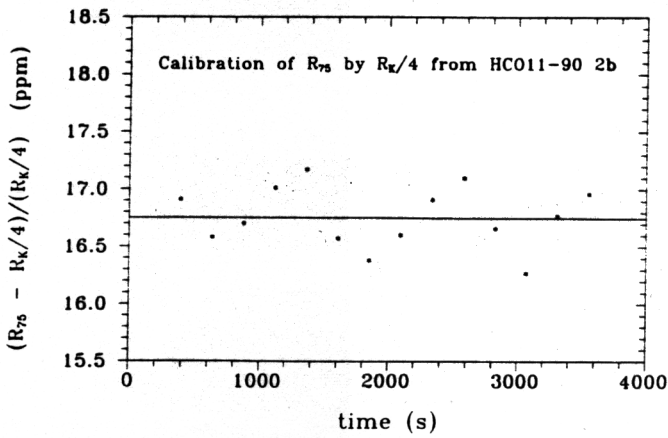


Fig. 9. The calibration of the standard wire wound resistor R_{75} from Fig. 8 shown here on an expanded scale. The mean value (shown as the horizontal line) yields the calibrated value of R_{75} in terms of the von Klitzing value. In Table I the calibrated values of our three wire wound standard resistors are tabulated referred to the temperature 23°C. The uncertainty indicated in Table I is dictated by the unstable temperature condition which the wire resistors experience.

crosses near the $+17 \times 10^{-6}$ mark. From Fig. 8 it is immediately seen that S is approximately -1.7×10^{-5} , this means that since $\delta I/I \cong 10^{-4}$, the term $S\delta I/I$ in eq. (10) is approximately -2×10^{-9} and hence negligible. It can also be seen from the figure that the peak-to-peak scattering of the values of S is of the order 10^{-6} . In Fig. 9 are shown 14 measured values of S . A calculation of the mean value yields the following calibration of R_w :

$$\frac{R_w - R_H(4)}{R_H(4)} = (16.7 \pm 0.1)10^{-6} - (0 \pm 2)10^{-11} \text{ s}^{-1} t \quad (11)$$

The quite high relative resolution of 10^{-7} in the calibration measurement is not equivalent with an uncertainty of 10^{-7} . This is because of large temperature fluctuations. Inside the shielded room the temperature in the range of 22°C to 25°C occasionally changes up to the order 1°C per hour. In order to make direct comparisons with other measurements the wire wound resistors all calibrations must be referred to the temperature 23.0°C. The uncertainty in the calibration of R_w is completely dominated by the uncertainty of the temperature of $\pm 1.5^\circ\text{C}$, which implies a total relative uncertainty of $\pm 1.5 \times 10^{-6}$ or $\pm 10 \text{ m}\Omega$.

In a comparison measurement standard resistors are measured at different laboratories, and the results compared to detect possible systematic errors. The standard resistors R_{75} , R_{76} , and R_{78} have been calibrated at three different laboratories, although not within very short time intervals. The three laboratories are: Tinsley, U.K. (30.09.88), the H. C. Ørsted Institute (23.08.90), and The Standards Laboratory of Scandinavian Airline System in Copenhagen, SAS (22.01.90). The results are given in Table I.

8. Concluding remarks

High resolution measurements of the resistivity at the centre of a Hall plateau on GaAlAs/GaAs heterostructure samples grown and processed at the H. C. Ørsted Institute have been demonstrated to be adequate for the purpose of quantum Hall calibration work. Calibration on an automated system has been performed, and hereby the system has

Table I. Three independent calibrations of three wire standard resistors from Tinsley. The three calibrations are done respectively at Tinsley, U.K., The Standards Laboratory of Scandinavian Airline Systems in Copenhagen (SAS) and at the H. C. Ørsted Institute against a quantum Hall resistor (HC011-90 2b). The temperature coefficient of the three wire-wound resistors, which is used, is measured by Tinsley.

$T = 296 \text{ K}$	R_{75}	R_{76}	R_{78}
Temp. coeff. [Ω/K]	-0.006	-0.008	-0.005
300988: Tinsley [Ω]	6453.182(32)	6453.142(32)	6453.225(32)
220190: SAS [Ω]	6453.323(13)	6453.186(13)	6453.351(13)
230890: HCØ [Ω]	6453.335(10)	6453.194(10)	6453.364(10)

turned out to have a relative resolution of the order 10^{-7} . The accuracy of the system has not yet been optimized. A professional properly tested calibration system is being built at the Danish Institute of Fundamental Metrology. However, calibration results of the standard resistors R_{75} , R_{76} , and R_{78} are on the 10^{-6} level confirming the calibration result obtained by the best Danish resistance calibration laboratory, SAS.

When reviewing the results two weak points in the system are particularly visible: the relatively bad current sources and the complete lack of thermal stabilization of the equipment kept at room temperature inside the shielded room. These two outstanding problems will definitely be improved in the next step in the development of a calibration facility. To link the system with the rest of the Danish calibration service is a question of comparing conventional 10 k Ω or 100 Ω standard resistors with the standard resistors of 6453.2 Ω calibrated as described above. Preliminary comparisons of 6.4 k Ω resistors with 10 k Ω resistors have been performed by connecting such two resistors in series. A current of e.g. 52.4 μA was passed through them, and by comparing the voltage drops of respectively 0.52 V and 0.34 V directly using DFMs automated 1 V Josephson array potentiometer the 10 k Ω resistor was calibrated in terms of the 6.4 k Ω resistor with a resolution of 1×10^{-7} . To compare the 6453.2 Ω resistor with a 100 Ω resistor is a little more complicated. Since now the ratio between the two resistors is 64 the Josephson array potentiometer cannot be used directly. This is because the relative noise level of the measurement on the 100 Ω resistor will be 64 times larger than on the 6453.2 Ω resistor preventing a relative resolution below 10^{-7} . Instead a Hamon bridge [19] consisting of eight 800 Ω resistors can be used. When the eight resistors in the bridge are coupled in series we have 6400 Ω nominally, and this can be calibrated against the 6453.2 Ω resistor using the Josephson array potentiometer directly. After this calibration the eight resistors are coupled in parallel now yielding a resistance 64 times lower than the one just calibrated. This ratio of 64 is determined better than 10^{-8} , when the relative resistances of the eight Hamon resistors are known better than 10^{-5} , because any relative deviation appears only in second order in the Hamon ratio. The final step is then to compare the 100 Ω resistor with the parallel coupled Hamon bridge using the Josephson array potentiometer. By implementing calibration schemes like this it seems possible that DFM very soon will be able to make absolute resistance calibrations of 100 Ω and 10 k Ω resistors limited only by the 2×10^{-7} built in relative uncertainty of

the quantum Hall resistor according to the international recommendations.

Acknowledgements

We are much indebted to C. B. Sørensen at the H. C. Ørsted MBE center for growing the MBE samples used in this investigation. A particular acknowledgement goes to A. Hartland at the NPL, England for his encouragement and help. The following colleagues have contributed to the described work: J. D. Ralston, K. Carneiro and J. U. Holtough. For technical assistance we thank M. Bøgelund-Jensen, J. Brinchman and C. Farver. The work has been supported by The Danish Science Research Council (11-4011), The Danish Metrology Council (1986-725/000-25) and The Danish Science Program for Materials Research ("Microstructures in III-V Semiconductors").

References

1. Taylor, B. N. and Witt, T. J. *Metrologia* **26**, 47 (1989).
2. Kibble, B. P., *Physica Scripta* **41**, 717 (1990).
3. Proceedings of the 12th Nordic Metrology Conference, 19-21 April 1989, Helsinki, Finland (Publisher: NORMET and WECC). See in particular the following articles: B. Nyruud: "Forandring av definisjonen for motstand, —praktisk betydning for industri og Kalibreringslaboratorier", J. Mygind: "Josephson junction voltage standard" and H. Bruus and P. E. Lindelof: "The quantum Hall resistor in Denmark".
4. Lampard, D. G. and Thomson, A. M., *Nature* **177**, 888 (1956).
5. Delahaye, F., *Metrologia* **25**, 73 (1988).
6. von Klitzing, K., Dorda, G. and Pepper, M. *Phys. Rev. Lett.* **45**, 494 (1980).
7. Cage, M. E., chapter 2 in *The Quantum Hall Effect* (Edited by R. E. Prange and S. M. Girvin), Springer Verlag, New York (1987).
8. Hartland, A., *Contemp. Phys.* **29**, 477 (1988).
9. Quinn, T. J., *Metrologia* **26**, 69 (1989).
10. Bruus, H., Ph.D. thesis "The QHE in GaAs/AlGaAs heterostructures, —Physical aspects and metrological applications", University of Copenhagen (1990).
11. Delahaye, F., *Metrologia* **26**, 63 (1989).
12. Giacomo, P., *Metrologia* **24**, 45 (1987).
13. Bruus, H. and Lindelof, P. E., *IEEE Trans. Instrum. Measurements*, **40**, 225 (1991).
14. Zhang, Z., Wang, D., Hu, Z., Zhen, J., He, Q., Blich, L., Hein, G., Kowalski, W., and Bruus, H., "A precise measurement of QHE in NIM", in *Proc. Conf. on Precision Electromagnetic Measurements CPEM '90*, Ottawa, Canada, June 11-14, 1990.
15. Nilsson, H., and Vallin, J., Statens Provningsanstalt, Sweden, Internal Report (1989).
16. Reedtz, G. M. and Cage, M. E., NIST preprint (1988).
17. Jucknischke, D., Buhlmann, H. J., Houdré, R., Ilegems, M., Py, M. A., Jeckelmann, B. and Schwitz, W., *IEEE Trans. Instrum. Measurements*, **40**, 228 (1991).
18. Cage, M. E., Field, B. F., Dziuba, R. F., Girvin, S. M., Gossard, A. C. and Tsui, D. C., *Phys. Rev.* **B30**, 2286 (1985).
19. Hamon, B. V., *Journ. Sci. Instr.* **31**, 450 (1954).